Electronic Supplementary Information

Heterogeneous NiS/NiO multi-shelled hollow microspheres with enhanced electrochemical performances for hybrid-type asymmetric supercapacitors

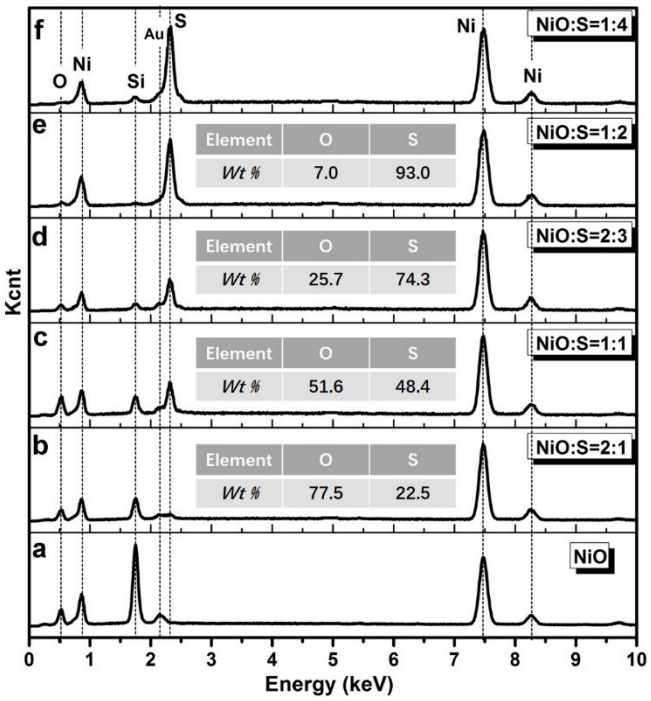

Fig. S1. The EDX spectra of the annealing products obtained from different ratio of NiO and S.

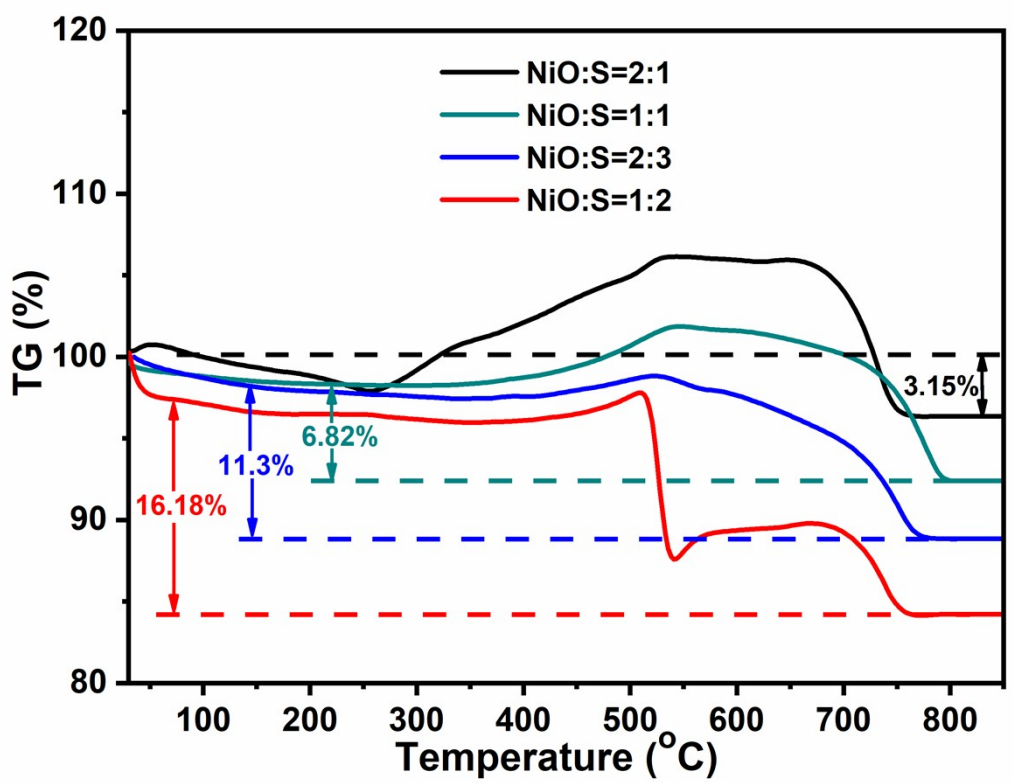

Fig. S2. TG curves of the nickel oxide/sulfide compounds. NiO can be oxidized to Ni_2O_3 at around 400 °C while Ni_2O_3 will decompose to NiO at higher temperatures. The final residues are all NiO for the tests.

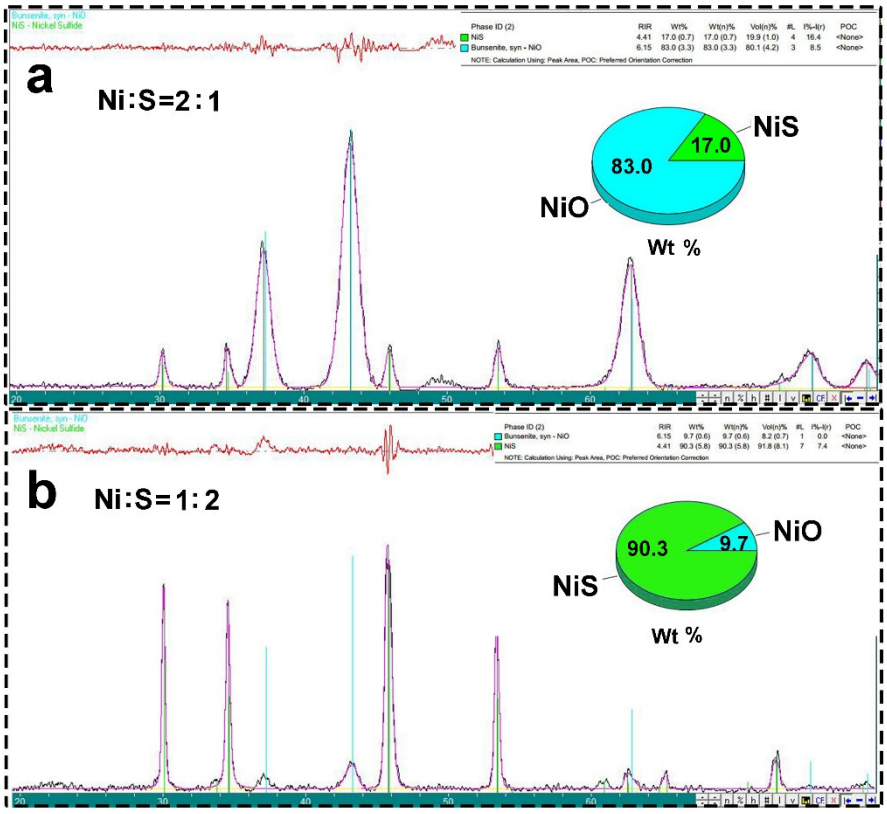

Fig. S3. The XRD analysis of two obtained samples when the mole ratio of 2:1, 1:2 (NiO:S) are applied.

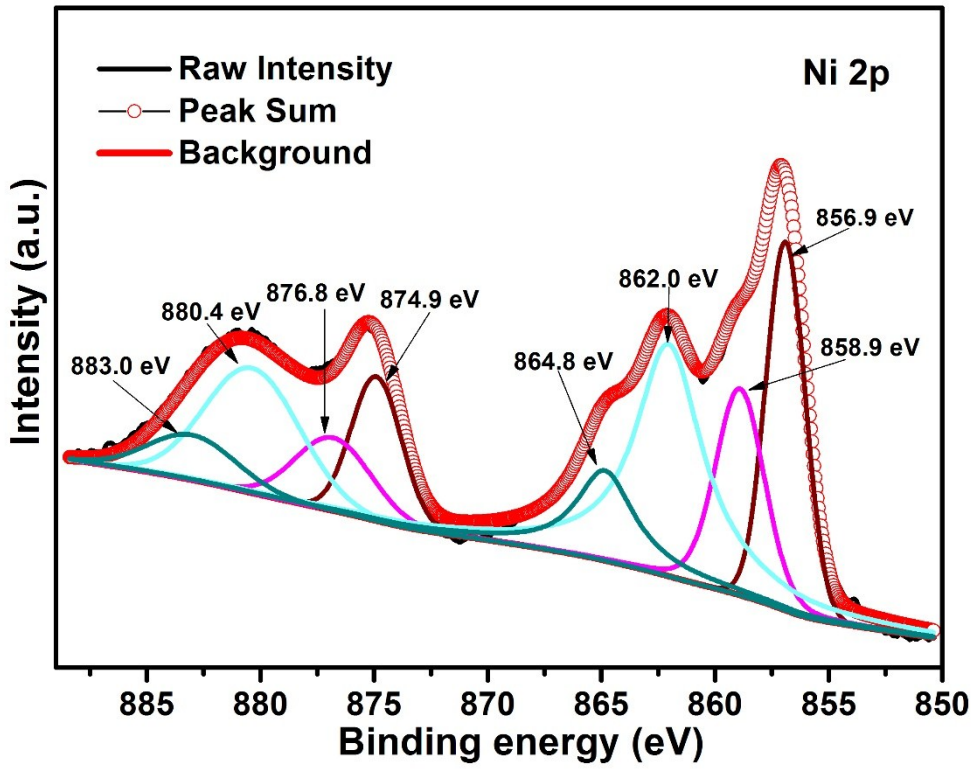

Fig. S4 XPS spectrum of Ni 2p of (NiO)0.1(NiS)0.9 multi-shelled hollow microspheres.

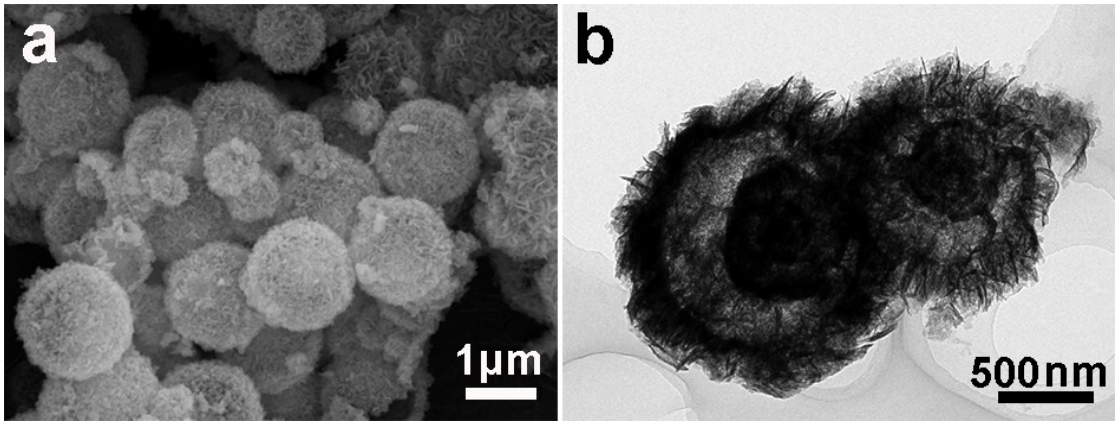

Fig. S5. SEM (a) and TEM (b) images of the multi-shelled $(NiO)_{0.85}(NiS)_{0.15}$ hollow microspheres.

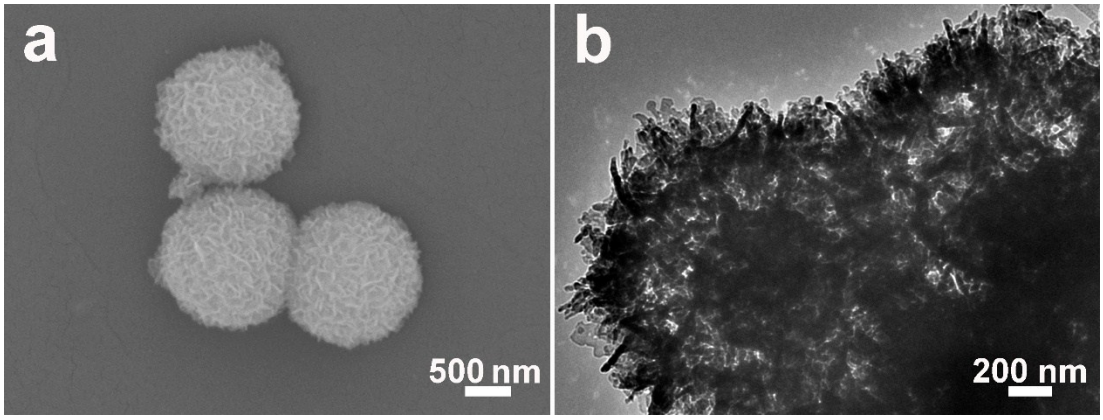

Fig. S6. SEM (a) and TEM (b) images of the multi-shelled $(NiO)_{0.65}(NiS)_{0.35}$ hollow microspheres.

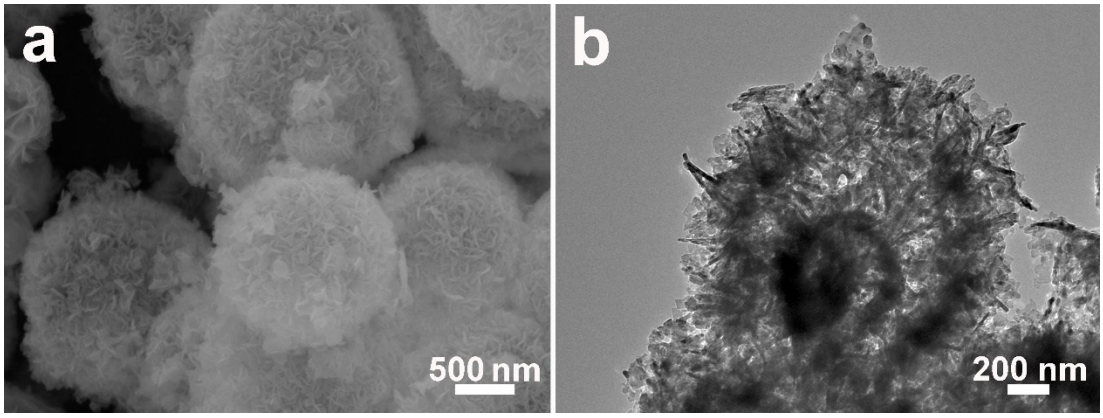

Fig. S7. SEM (a) and TEM (b) images of the multi-shelled $(NiO)_{0.4}(NiS)_{0.6}$ hollow microspheres.

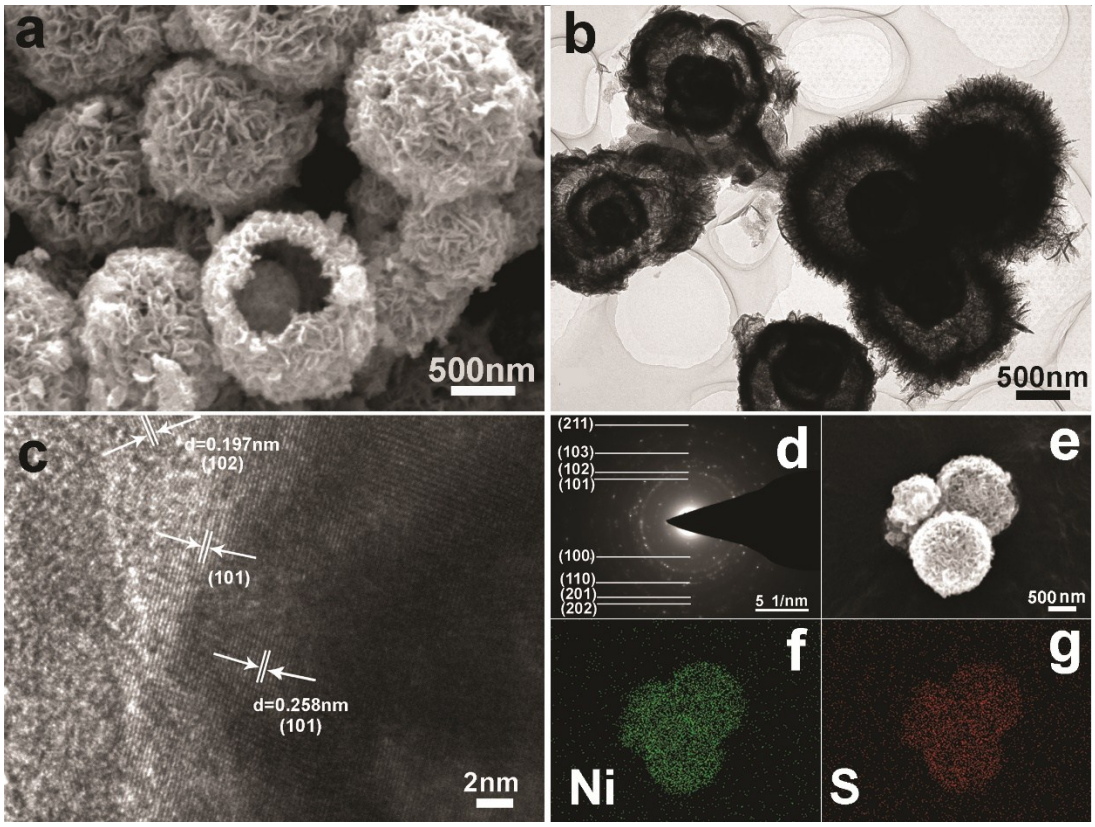

Fig. S8. SEM image (a), TEM image (b), HRTEM image (c), SAED patterns (d) and elemental mapping images (e-g) of the multi-shelled NiS hollow microspheres.

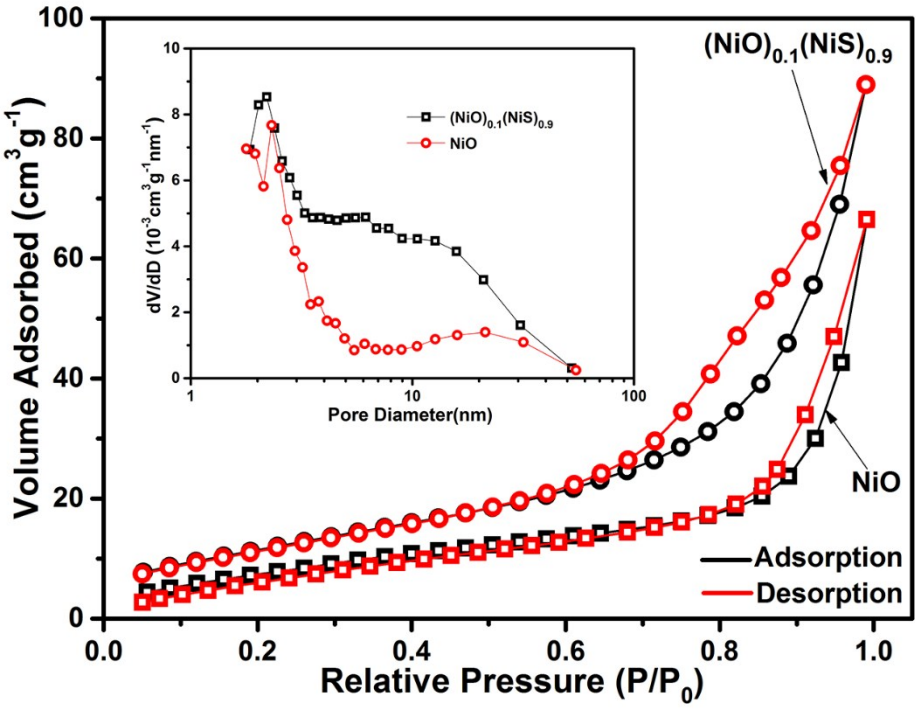

Fig. S9. Nitrogen adsorption-desorption isotherms and corresponding pore size distribution curves (the inset) of the NiO and $(NiO)_{0.1}(NiS)_{0.9}$ multi-shelled hollow microspheres.

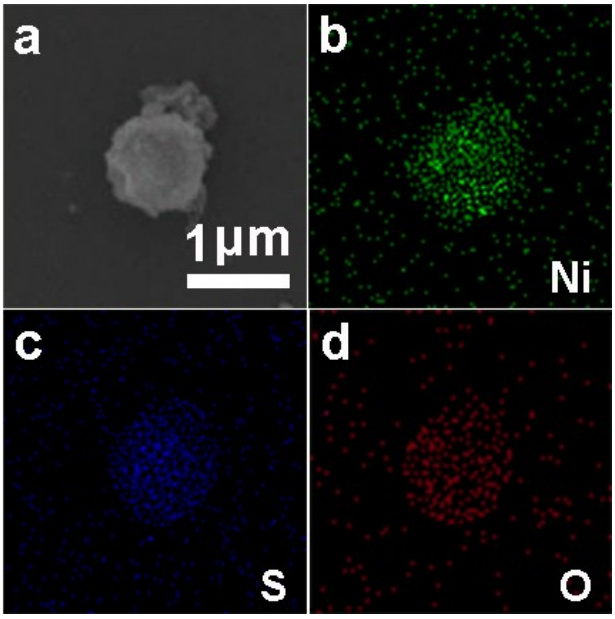

Fig. S10. Elemental mapping images (a-d) of $(NiO)_{0.1}(NiS)_{0.9}$ hollow microspheres.

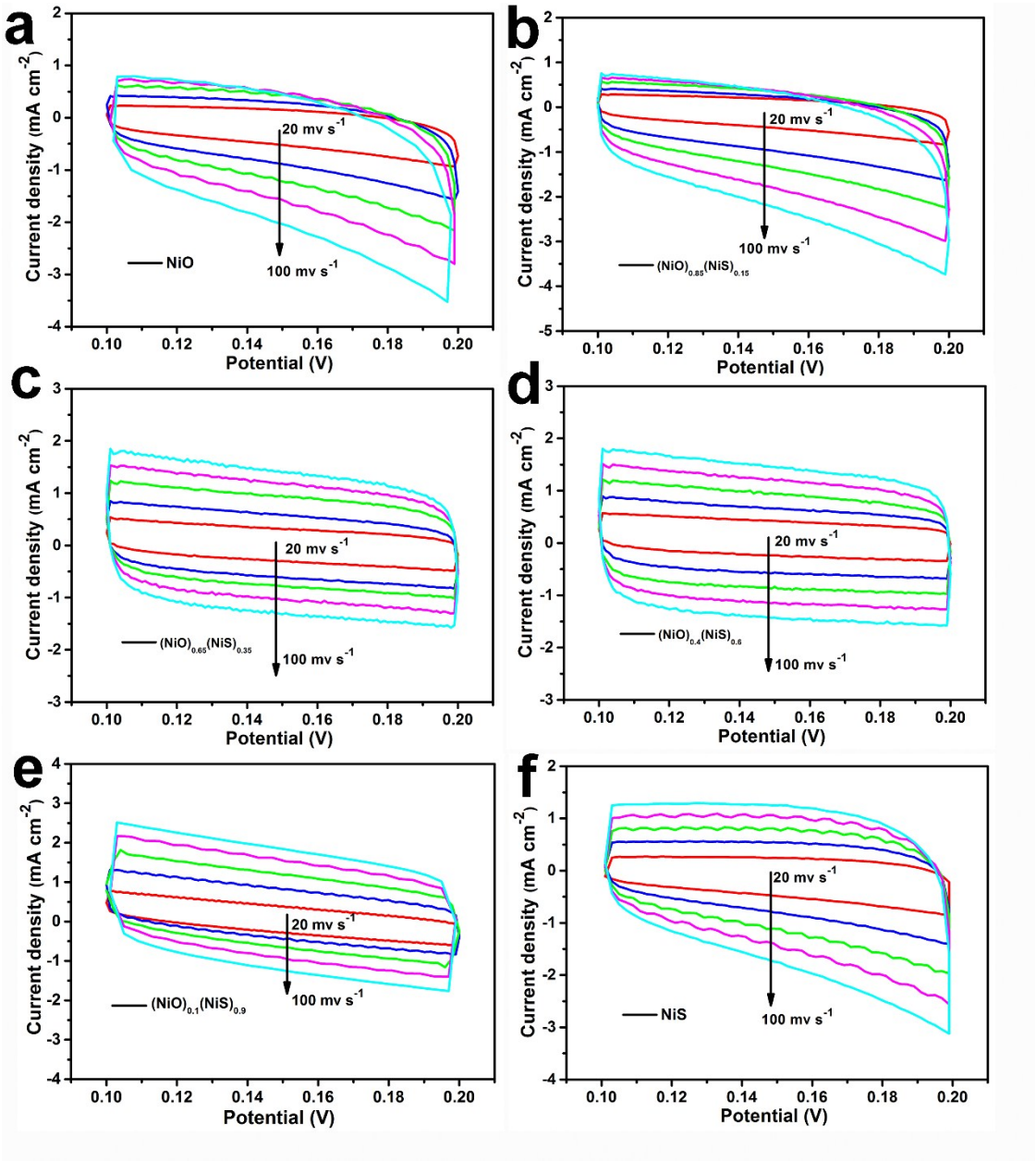

Fig. S11. CV curves of multi-shelled nickel-based hollow microspheres within a non-Faradaic potential window (*vs*. SCE) at different scan rates. (a) NiO, (b) $(NiO)_{0.85}(NiS)_{0.15}$, (c) $(NiO)_{0.65}(NiS)_{0.35}$, (d) $(NiO)_{0.4}(NiS)_{0.6}$,(e) $(NiO)_{0.1}(NiS)_{0.9}$ and (f) NiS.

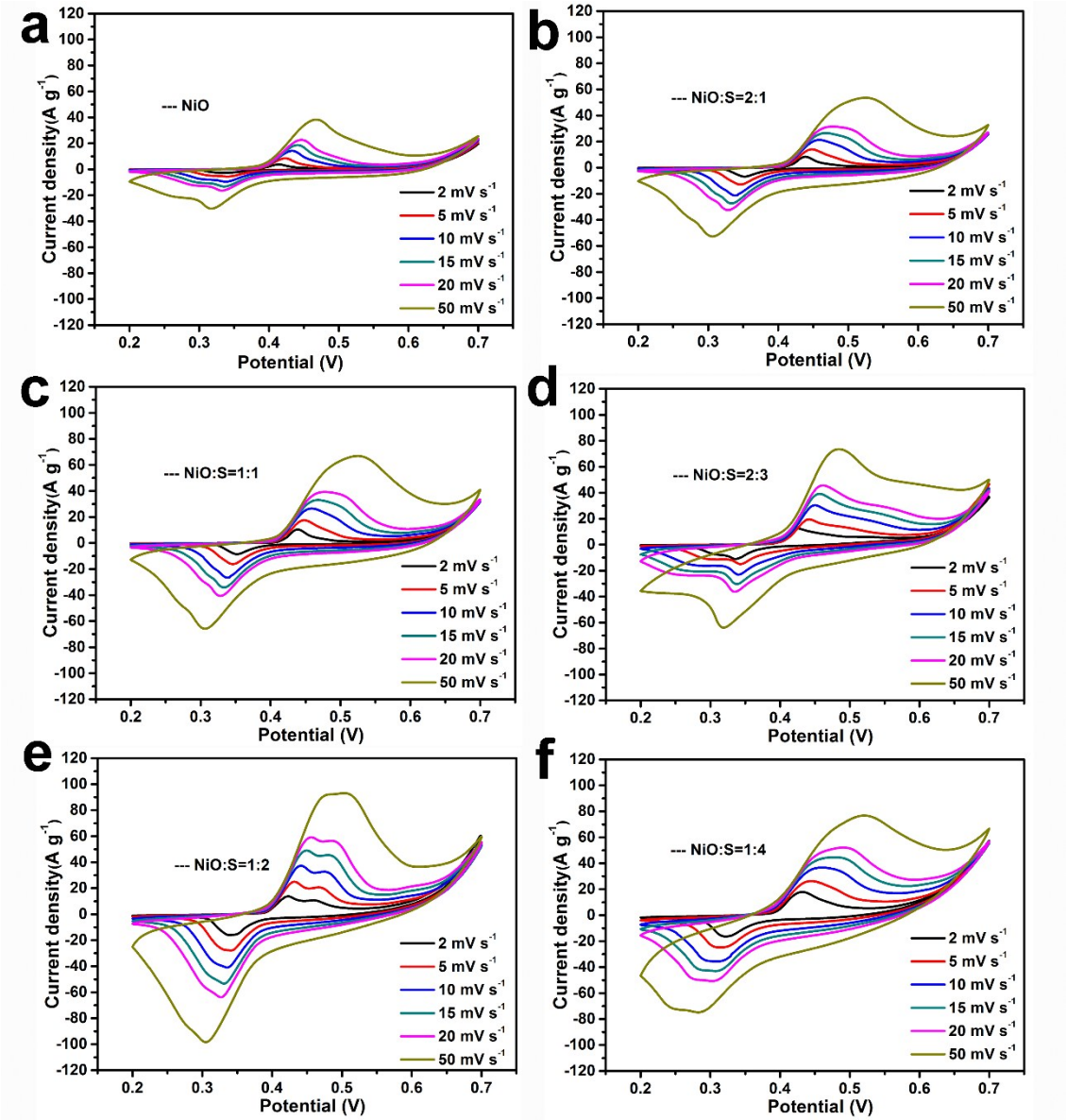

Fig. S12. CV curves performed at different scan rates of four samples. (a) NiO, (b) $(NiO)_{0.85}(NiS)_{0.15}$, (c) $(NiO)_{0.65}(NiS)_{0.35}$, (d) $(NiO)_{0.4}(NiS)_{0.6}$, (e) $(NiO)_{0.1}(NiS)_{0.9}$ and (f) NiS.

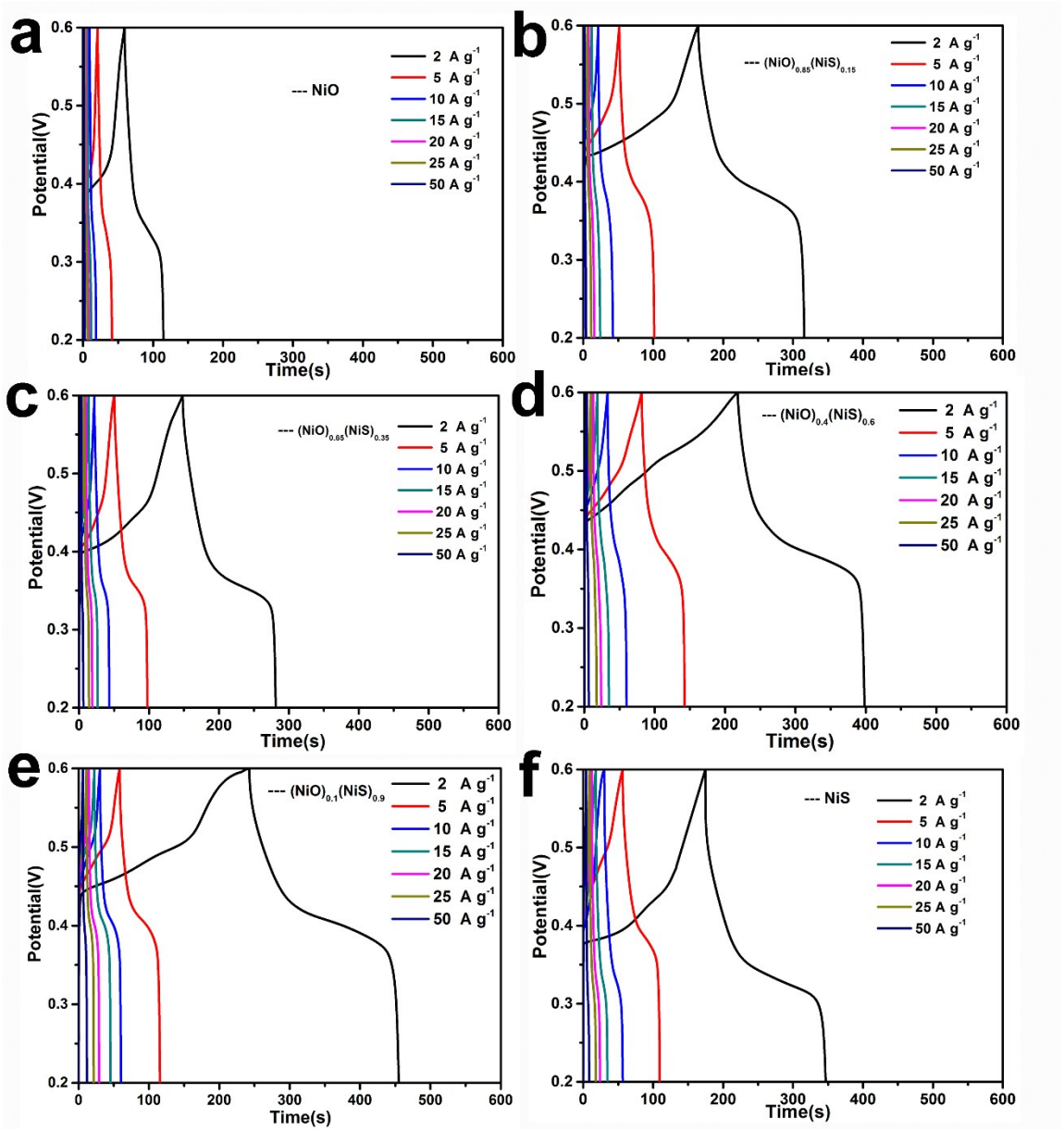

Fig. S13. The charge-discharge curves at different current densities of four samples. (a) NiO, (b) $(NiO)_{0.85}(NiS)_{0.15}$, (c) $(NiO)_{0.65}(NiS)_{0.35}$, (d) $(NiO)_{0.4}(NiS)_{0.6}$,(e) $(NiO)_{0.1}(NiS)_{0.9}$ and (f) NiS.

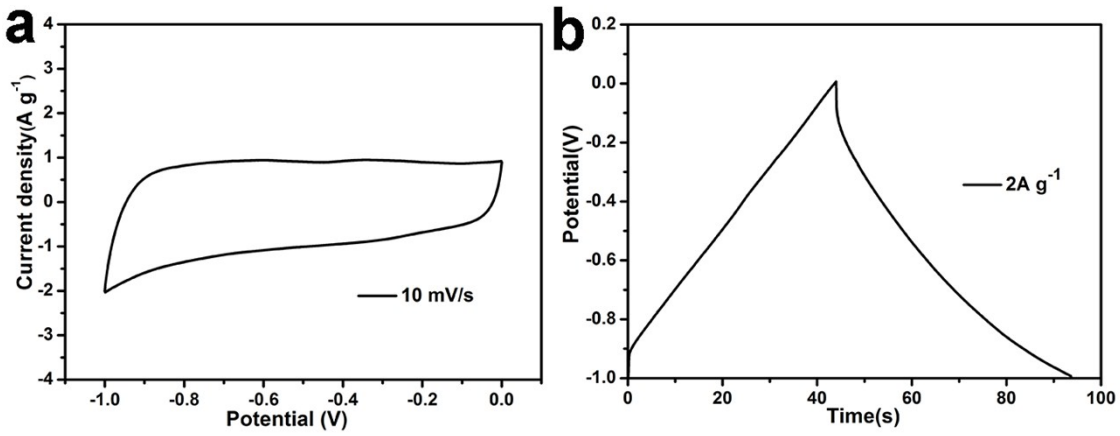

Fig. S14. CV curve at 10 mV s^{-1} (a) and the galvanostatic charge–discharge curve at current density of 2 A g^{-1} (b) of the AC electrode.